Chinese Chemical Letters 35 (2024) 108743

Contents lists available at ScienceDirect

Chinese Chemical Letters

journal homepage: www.elsevier.com/locate/cclet

Observation of high ionic conductivity of polyelectrolyte microgels in salt-free solutions

Qiangwei Wang[a,1], Huijiao Liu[a,1], Mengjie Wang[a], Haojie Zhang[a], Jianda Xie[b], Xuanwei Hu[a], Shiming Zhou[c], Weitai Wu[a,d,*]

[a] State Key Laboratory for Physical Chemistry of Solid Surfaces, Collaborative Innovation Center of Chemistry for Energy Materials, The Key Laboratory for Chemical Biology of Fujian Province, and Department of Chemistry, College of Chemistry and Chemical Engineering, Xiamen University, Xiamen 361005, China
[b] School of Materials Science and Engineering, Xiamen University of Technology, Xiamen 361024, China
[c] Hefei National Laboratory for Physical Sciences at the Microscale, University of Science and Technology of China, Hefei 230026, China
[d] School of Chemistry and Chemical Engineering, Ningxia University, Yinchuan 750021, China

ARTICLE INFO

Article history:
Received 6 March 2023
Revised 11 June 2023
Accepted 26 June 2023
Available online 27 June 2023

Keywords:
Polyelectrolhyte
Stimuli-responsive
Single-ion conducting
Liquid electrolyte
Lithium metal battery

ABSTRACT

Here, we report an observation that illustrate the potential of polyelectrolyte microgels in salt-free solutions to display a high ionic conductivity. Laser light scattering and ionic conductivity tests on very dilute aqueous dispersions of the microgels indicate that both small size and swollen state of gel particles play vital roles, which should favor the counterions to freely penetrate and leave gel particles, and thus can contribute to the ion-conducting property. Upon discovering this on microgels that are composed of imidazolium-based poly(ionic liquid), we also illustrate the generality of the finding to single lithium-ion polyelectrolyte microgels that are of more technically relevant features for applications, for instance, as injectable liquid "microgel-in-solution" electrolytes of high conductivity (*ca.* 8.2×10^{-2} S/m at 25.0 °C for 1.0×10^{-2} g/mL of microgels in a $LiNO_3$-free 1:1 v/v mixture of 1,2-dioxolane and dimethoxymethane) and high lithium-ion transference number (0.87) for use in the rechargeable lithium-sulfur battery.

Polyelectrolyte plays a crucial role in a wide range of fields across several disciplines, including biological processes, energy conversion, and information [1–3]. Besides the importance in science, with better understanding on how polyelectrolyte behaves, one is able to tune the physical properties to meet the application in rechargeable batteries, bioelectronics, and many others [3–8].

Because of the prospective applications, ionic conductivity of polyelectrolyte solutions has recently received an increased attention, which also is a primary means for characterizing the behavior of polyelectrolyte in solutions in that ionized counterions can dissolve into solvent as the mobile charge species at specific conditions [9–12]. Based on vast literature on experiments, theory and simulations, it is widely accepted that ionic conductivity of polyelectrolyte solutions is mainly determined by the electrostatic interactions, which can be mediated by the distribution of charged groups and charge density in polymer chains, polyelectrolyte concentration, counterion valence, solvent quality, ionic strength, and additional electrolyte ions in the solutions [3,4,9–12]. Despite the significant advances, many questions remain open. From an experimental point of view, studies on ionic conductivity of polyelectrolyte solutions typically focus on the polymers of a linear or branched structure, and their micro- and nano-structured aggregations as well, due to facile controllability of chain architectures. Yet, the behavior of polyelectrolyte in solutions is still very complicated, since it is a many-body problem. In salt-free solutions, theoretically, those polymer chains of a linear or branched architecture might aggregate to form microgel-like clusters [3,4,9,11]. Recent works tethered polyelectrolyte chains on inorganic particles [13–18]. However, comparably little attention is paid on ionic conductivity of microgels of an internally chemically-crosslinked structure. While polyelectrolyte microgels with finite size have been synthesized by top-down or bottom-up strategies [19–21], so far, there is rare report that referred to high ionic conductivity of such microgels in salt-free solutions.

In this manuscript, we would like to report an investigation on ionic conductivity of polyelectrolyte microgels, consisting of poly(ionic liquid) (PIL). PIL is a class of polyelectrolytes that comprises ionic liquid (IL) species as repeating electrolyte units, which makes it combine the characteristic properties of both polymers

* Corresponding author at: College of Chemistry and Chemical Engineering, Xiamen University, Xiamen 361005, China.
E-mail address: wuwtxmu@xmu.edu.cn (W. Wu).
[1] These authors contributed equally to this work.

https://doi.org/10.1016/j.cclet.2023.108743
1001-8417/

and ILs [22–24]. PIL has also been made into gels, introducing extra advantages in terms of functionality, elasticity and scalability [22–24]. Different from polyelectrolytes in salt-free solutions, the macroscopic or bulky gel analogies containing the solvent as a whole are typically considered as electrostatically neutral, and consequently microscopic gels sometimes are assumed to be electrically neutral [3,4,9–11]. On the contrary, a pioneering simulation work predicts that the microscopic gels of size smaller than *ca.* 250 nm may not confine the counterions completely [25]. Inspired by this, one wonders if it is possible to observe high ionic conductivity of polyelectrolyte microgels in salt-free solutions. As a proof of the concept, herein we show it on the starting microgels of imidazolium-based PIL and poly(tetrabutylphosphonium 4-styrenesulfonate) (pTPSS), which exhibits a lower critical solution temperature (LCST) in water that can be exploited in developing stimuli-responsive materials [26–28], and also on the extending microgels of other PILs (Fig. 1). Furthermore, with a structure similar to the emerging "localized high-concentration electrolytes" in lithium metal batteries [29,30], we speculate that the microgels may serve as injectable liquid "microgel-in-solution" electrolytes.

We initially prepared pTPSS microgels in water (25.0 mL) by free radical polymerization of tetrabutylphosphonium 4-styrenesulfonate (TPSS; 1.8×10^{-3} mol; Fig. S1 in Supporting information) with 1,6-dialkyl-3,3′-bis-1-vinyl imidazolium bromide as an IL cross-linker ($[C1,6(Vim)_2]Br$; 7.3×10^{-5} mol; Fig. S2 in Supporting information), and 2,2′-azobis(2-methylpropionamidine) dihydrochloride (AAPH; 1.1×10^{-4} mol) as an initiator, in the presence of surfactant cetyl trimethyl ammonium bromide (CTAB; 2.0×10^{-5} mol) under N_2 purge at 70.0 °C (see Supporting information for the details). pTPSS is thermo-sensitive, allowing the synthesis of monodisperse pTPSS-based microgels with controllable size from well-established precipitation polymerization [19–21]. It is possible that pTPSS becomes hydrophobic relatively to enable the formation of gel particles at temperatures above its LCST [26–28], resulting in the spherical-like microgels (collected after reacting for 5 h, and purified before tests; Fig. 2a). In IR analysis (Fig. S3 in Supporting information), characteristic bands of skeletal vibration (*ca.* 1181 and 1451 cm^{-1}) for imidazole rings of $[C1,6(Vim)_2]Br$ units [31], and the bands of sulfonate asymmetrical (*ca.* 1217 cm^{-1}) and symmetrical stretching vibration (*ca.* 1036 cm^{-1}) for sulfonate groups [26–28] of TPSS units, were detected. Microgels were hydrophilic (Fig. S4 in Supporting information), and kept stable in water for at least 3 months without significant change in the average hydrodynamic radius $<R_h>_0$ (*i.e.*, "equivalent sphere radius" produced by an angular extrapolation of apparent diffusion coefficient of microgels, Fig. S5 in Supporting information), as measured by dynamic light scattering (DLS) under N_2 atmosphere (the same below). To verify both the composition and the hydrophilicity, 10 more samples were synthesized (Table S1 in Supporting information) with varied feeding concentrations of CTAB ([CTAB]), which leaded to samples of different sizes with $<R_h>_0$ in the range of 34–326 nm (measured in water at 25.0 °C, Fig. 2b), whereas of similar water absorbency (*ca.* 320-folds against dried samples; Fig. S6 in Supporting information) and of similar polymer density (*ca.* 0.003 g/cm^3; Fig. S7 in Supporting information). Microgels can be reproduced from batch to batch, with an average yield of *ca.* 92% (Table S1).

The ion-conducting property for pTPSS microgels in very dilute aqueous dispersion (0.025 wt%) was assessed by AC impedance system equipped with a temperature controller (±0.1 °C), under N_2 atmosphere. The selection of such a low concentration below 0.1 wt% was to conserve individuality of microgels [32], which had been confirmed by freely diffusive motion of microgels in the particle dynamics test by using diffusing wave spectroscopy (Fig. S8 in Supporting information) [33]. The fluctuation on viscosity for such dispersions of different microgels is also ignorable [34]. The data in Fig. 2c display the surprising result that for microgels of the smallest size ($<R_h>_0$ of 34 nm), an ionic conductivity (σ_{ionic}) of 7.1×10^{-5} S/m was observed for the very dilute aqueous dispersion at 25.0 °C. It appears, however, that as the size of microgels increased in the $<R_h>_0$ range of 34–326 nm, σ_{ionic} decreased and then flatted off. Typically, for microgels of $<R_h>_0 \geq 167$ nm, σ_{ionic} of $\leq 1.3 \times 10^{-5}$ S/m was obtained. Overall, the observation seems to agree with the simulation-based prediction reported earlier [25].

We tentatively ascribe the observed σ_{ionic} to counterions that are free to penetrate and leave gel particles, owing to the discretization of charges according to the investigation by a combined simulational model and Poisson–Boltzmann theory [25]. Considering that ion dissociation is not likely (or minimal at least) to occur

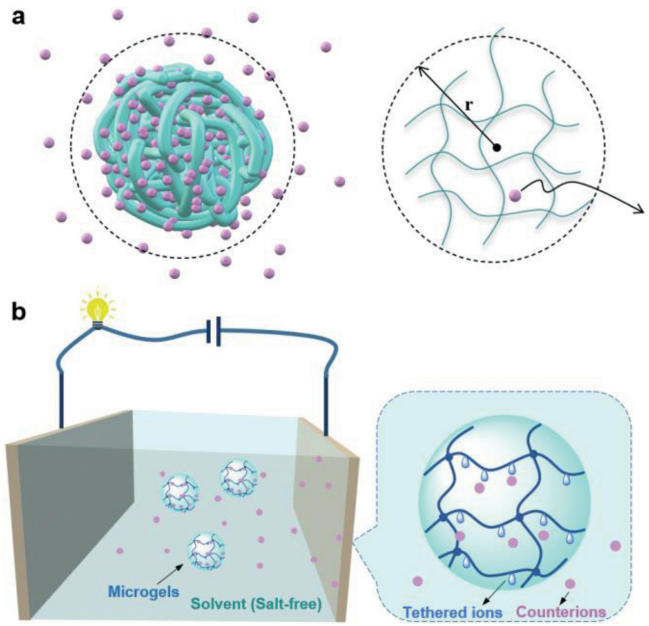

Fig. 1. Illustration for (a) the discretization of counterions from gel particles according to an earlier study by a combined simulational model and Poisson–Boltzmann theory [25], and (b) polyelectrolyte microgels in salt-free solution as an injectable microgel-in-solvent system of a high ionic conductivity in this work.

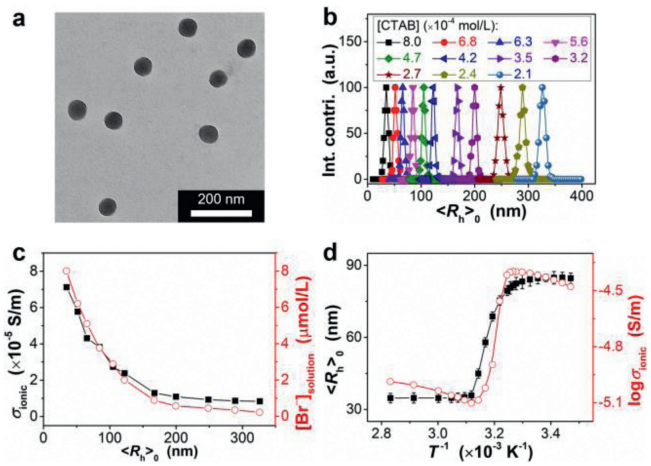

Fig. 2. Results of pTPSS microgels. (a) A typical TEM image. (b) DLS size distribution of microgels prepared with the varied [CTAB], and (c) the σ_{ionic} and $[Br^-]_{solution}$ as a function of $<R_h>_0$ of those microgels. (d) Temperature dependence of $<R_h>_0$ and $\log\sigma_{ionic}$ of a selected microgel sample (CM-4).

for TPSS units with large cations containing tetrabutyl chains (Fig. S9 in Supporting information) [35–37], it is plausible that σ_{ionic} is mainly related to Br^- ion, originating from ion dissociation in $[C1,6(Vim)_2]Br$ units that may be easier to occur [35,36]. To this end, microgel dispersions in equilibrium state were separated by using dialysis membrane, and the solutions were collected for examining the concentration of Br^- ion ($[Br^-]_{solution}$) by inductively coupled plasma–atomic emission spectroscopy. For the dispersion of microgels with $<R_h>_0$ of 34 nm, the $[Br^-]_{solution}$ was estimated to be *ca.* 8.0×10^{-6} mol/L, which is approximately 36 mol% among total Br^- ions in the system; that is, the mol fraction of Br^- ion inside gel particles was only 64 mol% (Fig. S10 in Supporting information), confirming a high permeability of microgels to allow the counterions to freely penetrate and leave the gel particle. If the diffusion coefficient of Br^- ion is assumed to be 2.0×10^{-9} m^2/s [38], the Nernst-Einstein conductivity [39] is *ca.* 6.0×10^{-5} S/m, which is close to the observed σ_{ionic}. The deviation of the Nernst-Einstein conductivity from the observed σ_{ionic} is likely due to the difficulty to fully collect the counterions in solutions, particularly those located in vicinity of tethered cations [3,4,9–11], and the inevitable escape of Br^- from microgels during their purification. Nevertheless, this result well connects the observed σ_{ionic} to $[Br^-]_{solution}$. As shown in Fig. 2c, $[Br^-]_{solution}$ decreased as the size of microgels increased in the experimental $<R_h>_0$ range of 34–326 nm, which mirrors that of the observed σ_{ionic} evolution along with microgel size. This relationship can serve as a further support on the interpretation that the σ_{ionic} is attributed to the counterions that can penetrate and leave gel particles. Moreover, compared to the time scale for diffusion of counterions, it is long for gel particles according to the Stokes-Einstein equation [39], which can be considered to be immobile [40] and thus contribute minimal to σ_{ionic}.

Because pTPSS is thermo-sensitive [26,27], the size of pTPSS microgels should be varied by heating [28]. Microscopically, there is an analogy between the "coil-to-globule" transition of a single linear polymer chain and the volume phase transition (rendering the size change) of a polymer gel, and the swelling or shrinking of a polymer gel may be viewed as a consequence of the expansion or contraction of subchains between two neighboring cross-linking points inside the polymer gel network (Fig. S11 in Supporting information) [26–28]. Fig. 2d shows DLS data on the temperature-dependent $<R_h>_0$ of a selected microgel sample (0.025 wt% in water and $<R_h>_0$ of 85 nm at 25.0 °C; CM-4 in Table S1). The $<R_h>_0$ decreased gently with temperature until a shaper volume change from the swollen to collapsed state, and then flatted off above 47.5 °C, showing a LCST-type thermo-induced swelling-deswelling transition of volume phase transition temperature (VPTT) appearing at *ca.* 42.6 °C (as estimated from an asymmetric Lorentz fit of first derivative of $<R_h>_0$, Fig. S12 in Supporting information). Thus, this microgel sample offered different sizes of different compressabilities to investigate the generality of the ion-conducting property. The ionic conductivities σ_{ionic} as a function of temperature for the microgel sample in water are presented in Fig. 2d, and it is interesting to note that the ionic conductivities σ_{ionic} obtained at different temperatures did not exhibit a typical dependence on temperature. Instead of a linear relationship between $\log\sigma_{ionic}$ and T^{-1}, three regions can be distinguished roughly in this plot: at low temperatures of <33.0 °C, σ_{ionic} increased slightly; in the region of *ca.* 33.0–47.5 °C, however, σ_{ionic} decreased as temperature increased, showing a local minimum around the VPTT of microgels; finally, at >47.5 °C, σ_{ionic} increased again with temperature. In particular, when compared to the data for fully swollen microgels (at <33.0 °C), fully collapsed microgels (at >47.5 °C) had smaller $<R_h>_0$, but overall exhibited lower σ_{ionic}. We attributed this observed $\log\sigma_{ionic}$-T^{-1} relationship mainly to the impact of the swollen/collapsed state of microgels on the leakage of counterions from gel particles: (i) the thermo-induced phase transition from the swollen to collapsed state could lead to higher polymer density (and thereby cation density) of gels [40–42], which likely results in stronger anion–cation electrostatic interactions [3,4,9–11]; (ii) when gel particles shrink to some extent, the surface may form a relatively tough skin [43], which likely results in increased steric hindrance [3,4,9–11]. Both these factors can hinder the leakage of counterions from gel particles, in agree with what was observed (Fig. S13 in Supporting information). In addition, although the change in the ion dissociation may also affect the σ_{ionic} and it has also been reported to decrease with increasing temperature, in general, these effects are found to be minimal for IL/solvent systems in our experimental temperature range and thus should be negligible [35–37]. In <33.0 °C region and >47.5 °C region, respectively, where $<R_h>_0$ of microgels stayed almost constant, the increase in segmental dynamics with temperature dominated that improved ion transport, σ_{ionic} raised with temperature of Vogel–Fulcher–Tammann-like dependence [3,4,9–11]. Similar phenomenon was registered for other microgel samples (*e.g.*, CM-2 and CM-6 in Table S1, Fig. S14 in Supporting information). Thus, these results suggest that the presented microgels in salt-free solutions can combine within a single object both the ionic conductive character of polyelectrolyte in solutions and the stimuli-responsive character of gels, allowing manipulating ion-conducting property *via* tuning the swollen/collapsed states of gel particles as well.

To further examine the impact of the swollen/collapsed states of gel particles on the ion-conducting property of PIL microgels, and also to generalize the finding to other PIL microgels, pTPSS-VPBA microgels were prepared on the basis of pTPSS microgels through functionalization with phenylboronic acid group (PBA) by additional feeding 4-vinylphenylboronic acid (VPBA) in microgel synthesis (Fig. S15 in Supporting information). Under our testing conditions (pH 4.5 at 25.0 °C under N_2 atmosphere, for the 0.025 wt% dispersion of pTPSS-VPBA microgels), VPBA groups were mainly in uncharged form (Fig. S16 in Supporting information), which can react with *cis*-diols (glucose herein) that leads to thermodynamically more favorable charged form, and thereby alter the polymer-solvent affinity form a hydrophobic character to relatively more hydrophilic [44,45]. For microgels of PBA content above 15 mol% (24 mol% for pTPSS-VPBA microgels), one glucose molecule can bind with two PBA groups to form glucose-bis-boronic complex at low temperatures, which would break down by heating and the formation of monobidentate is favored at relatively high temperatures (Fig. S17 in Supporting information) [44,45]. Since thermo-induced (de)swelling characteristics is a consequence of the balance of expanding and shrinking forces in microgels at particular temperatures [40–42], the competition between the formation of bis-bidentate (rendering shrinking) and its breakdown to form monobidentate (rendering expanding) could lead to a switch in gel volume phase behavior (Fig. 3a) from LCST-type (with glucose concentration of $[Glu] \leq 2.0 \times 10^{-3}$ mol/L) to thermo-unsensitive ($2.0 \times 10^{-3} < [Glu] < 4.0 \times 10^{-3}$ mol/L), then in reverse ($[Glu] \geq 4.0 \times 10^{-3}$ mol/L) to exhibit an upper critical solution temperature (UCST), and thus offered three sample types of three different thermo-induced swelling-deswelling transition behaviors to clarify the generality. For microgel dispersion with a [Glu] of 1.0×10^{-3} mol/L (Fig. 3b), the $\log\sigma_{ionic}$–T^{-1} profile agreed well with that for pTPSS microgels (Fig. 2d), and around the VPTT of microgels the σ_{ionic} displayed a local minimum. The $\log\sigma_{ionic}$–T^{-1} plot showed Vogel–Fulcher–Tammann-like dependence at [Glu] of 3.0×10^{-3} mol/L (Fig. 3c), and a three-step increase roughly with temperature at a higher [Glu] of 6.0×10^{-3} mol/L (Fig. 3d), which well reflected the glucose-tuned evolution of thermo-induced swelling–deswelling transition behaviors of pTPSS-VPBA microgels. These results confirmed that the swollen state of gel particles plays a vital role, and the higher σ_{ionic} could be obtained when micro-

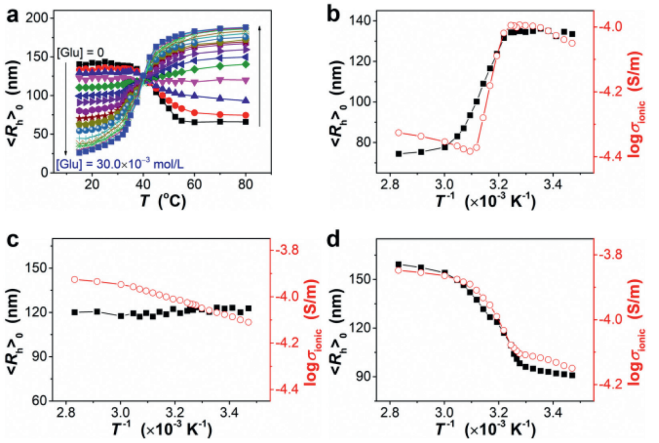

Fig. 3. Results of pTPSS-VPBA microgels. (a) The $<R_h>_0$ as a function of temperature in the presence of glucose of different [Glu]s, in the [Glu] range of 0–30.0×10^{-3} mol/L with an interval of 1.0×10^{-3} mol/L for the range from 0 to 10.0×10^{-3} mol/L, 2.0×10^{-3} mol/L for the range from 10.0×10^{-3} to 14.0×10^{-3} mol/L and 4.0×10^{-3} mol/L for the range from 14.0×10^{-3} to 30.0×10^{-3} mol/L. (b-d) Temperature dependence $<R_h>_0$ and $\log\sigma_{ionic}$ at a [Glu] of (b) 1.0×10^{-3} mol/L, (c) 3.0×10^{-3} mol/L, and (d) 6.0×10^{-3} mol/L.

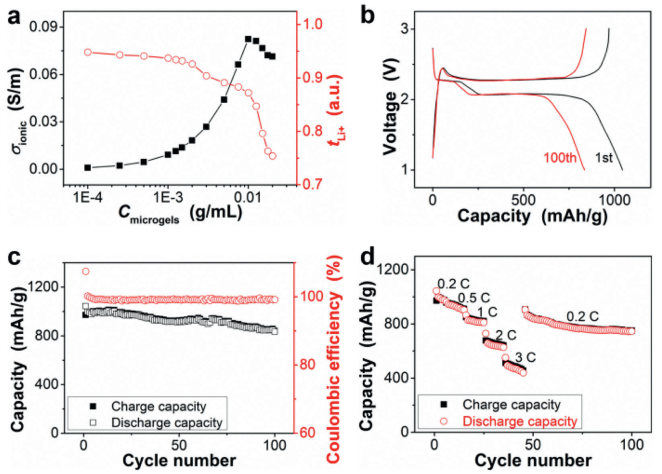

Fig. 4. Results of pLiMTFSI microgels. (a) The σ_{ionic} (■) and the t_{Li^+} (○) at 25.0 °C as a function of $C_{microgels}$ in $LiNO_3$-free DOL/DME. (b-d) The electrochemical performance of Li–S battery, with microgels in DOL/DME of $C_{microgels}$ of 1.0×10^{-2} g/mL as liquid electrolyte: (b) charge/discharge profiles and (c) cycle life of charge/discharge capacities and the Coulombic efficiency at a rate of 0.2 C, and (d) charge/discharge capacities at various current densities.

gels were in a relatively swollen state, relative to their collapsed state.

Having observed that the ion-conducting property of PIL microgels in salt-free solutions is related to the size and the swollen/collapsed states of gel particles, we further investigated the generality of the finding to microgels with more technically relevant features for applications as injectable "microgel-in-solution" electrolytes (Fig. S18 in Supporting information), for instance, in the rechargeable batteries. Such "microgel-in-solution" electrolytes remind us of "localized high-concentration electrolytes" [29,30]. With a similar structure, we speculate that the microgels might be used in lithium metal batteries. To this end, Li–S batteries with a low sulfur loading (*ca.* 1 mg/cm^2) were employed as a simplified model with less complex environment to validate the possibility of "microgel-in-solution" as electrolyte, because a high sulfur loading may give rise to fast lithium anode corrosion accompanied by side reactions [46], although a sulfur loading of higher than 6 mg/cm^2 is usually needed to meet the energy density requirement for vehicular applications at the pack level [47,48]. In this case, to combine in the same microgels the two contributions (small and swollen), pLiMTFSI microgels with $<R_h>_0$ of 17 nm in the swollen state in a mixture of dimethoxymethane (DME) and 1,2-dioxolane (DOL) (1:1 in volume) at 25.0 °C (Fig. S19 in Supporting information) were prepared by polymerization of commercially available monomer lithium 1-[3-(methacryloyloxy)propylsulfonyl]−1-(trifluoromethanesulfonyl)imide (LiMTFSI), and ethylene glycol dimethacrylate and divinylbenzene as crosslinkers [49]. It can be seen in Fig. 4a that the σ_{ionic} displayed a non-monotonic dependency on the concentration of microgels ($C_{microgels}$) in $LiNO_3$-free DOL/DME. Not surprisingly, while polymer crews are well separated and interactions between them are negligible in the very dilute regime of the same solvent [32], the σ_{ionic} increased gently with increasing $C_{microgels}$, due to the increase in $C_{microgels}$ and thus the concentration of free ions (lithium-ion, Li^+, herein). At the higher $C_{microgels}$ of above *ca.* 2.0×10^{-3} g/mL (*i.e.*, 0.2 wt%), polymer crews not only have strong interactions but might also have enough freedom to form aggregates [32,33], leading to the screening of electrostatic interactions among polymer crews that can make additional contribution to the increase in σ_{ionic} *via* the increase in mobility of charge carriers [3,4,9–11]. Meanwhile, gel particles might approach each other closer with increasing $C_{microgels}$, leading to entangling among the surface of those neighboring particles that can reduce mobility of cations compared to that in non-entangled surface region [3,4,9–11,31]; the viscosity of microgel dispersion has been documented to increase with increasing the concentration of microgels [34], which can also reduce mobility of the cations [39]. As a result of competitive effects on the concentration and the mobility of free ions, the σ_{ionic} reached a maximum of *ca.* 8.2×10^{-2} S/m at $C_{microgels}$ of 1.0×10^{-2} g/mL (the $[Li^+]_{solution}$ was estimated to be *ca.* 2.1×10^{-2} mol/L, which is approximately 81 mol% among total Li^+ ions in the system) at 25.0 °C, which meets the requirement (*ca.* 10^{-2} S/m) [47,48] for commercial applications. The above explanation is supported by an estimation on the molar ionic conductivity, which was estimated by the ratio of the σ_{ionic} and the monomeric concentration of LiMTFSI in dispersion (Fig. S20 in Supporting information) [3,4,9–11]. Furthermore, because of the large difference in the size, and thus mobility, of Li^+ ion and its counterions (tethered to microgels), it is reasonable that a high Li^+ transference number ($t_{Li^+} \geq 0.87$; Fig. 4a and Fig. S21 in Supporting information) can be reached at $C_{microgels}$ of $\leq 1.0 \times 10^{-2}$ g/mL at 25.0 °C; even at $C_{microgels}$ of $>1.0 \times 10^{-2}$ g/mL, it retains considerable high t_{Li^+} of >0.75, which still remains superior to most liquid electrolytes [10,50–52]. These results indicated that such PIL microgels in salt-free solutions are a promising route to a high conductivity, high transference number electrolyte, which presents the possibility of incorporating directly to current cells without significant redesign of electrode formulations (Figs. 4b-d and Table S2 in Supporting information).

In summary, we have observed phenomena that illustrate the potential ability of polyelectrolyte microgels in salt-free solutions to show a high ionic conductivity. The observation should be rationalized by considering both small size and swollen state of microgels, which favor counterions to freely penetrate and leave gel particles, and serve as the mobile charge carriers that would contribute to the ion-conducting property. Achieving a high conductivity on polyelectrolyte microgels in salt-free solutions is not only of fundamental interest, but is also promising in terms of paving the way to a broad range of technical applications, for example, toward advanced liquid electrolytes for better batteries.

Declaration of competing interest

The authors declare that they have no known competing financial interests or personal relationships that could have appeared to influence the work reported in this paper.

Acknowledgments

This work is supported by National Natural Science Foundation of China (Nos. 21774105 and 20923004), Chuying Plan Youth Top-notch Talents of Fujian Province, and National Fund for Fostering Talents of Basic Science (No. J1310024).

Supplementary materials

Supplementary material associated with this article can be found, in the online version, at doi:10.1016/j.cclet.2023.108743.

References

[1] H.W. Xia, Y. Hou, T. Ngai, et al., Phys. Chem. B 114 (2010) 775–779.
[2] Q.W. Bai, X. Chen, J.X. Chen, et al., ACS Macro Lett. 11 (2022) 1107–1111.
[3] M.A. Muthukumar, Macromolecules 50 (2017) 9528–9560.
[4] A.V. Dobrynin, R.H. Colby, Macromolecules 28 (1995) 1859–1871.
[5] K. Achazi, R. Haag, M. Ballauff, et al., Angew. Chem. Int. Ed. 60 (2021) 3882–3904.
[6] L.L. Zhao, M. Skwarczynski, I. Toth, A.C.S. Biomater, Sci. Eng. 5 (2019) 4937–4950.
[7] A.M. Rumyantsev, N.E. Jackson, J.J. de Pablo, Annu. Rev. Condens. Matter Phys. 12 (2021) 155–176.
[8] X.Y. Fan, C. Zhong, J. Liu, et al., Chem. Rev. 122 (2022) 17155–17239.
[9] C. Cametti, Polymers 6 (2014) 1207–1231.
[10] K.M. Diederichsen, E.J. McShane, B.D. McCloskey, ACS Energy Lett. 2 (2017) 2563–2575.
[11] V. Bocharova, A.P. Sokolov, Macromolecules 53 (2020) 4141–4157.
[12] J. Park, A. Staiger, S. Mecking, K.I. Winey, ACS Macro Lett. 11 (2022) 1008–1013.
[13] Y.Y. Lu, S.K. Das, S.S. Moganty, et al., Adv. Mater. 24 (2012) 4430–4435.
[14] Y.Y. Lu, K. Korf, Y. Kambe, et al., Angew. Chem. Int. Ed. 53 (2014) 488–492.
[15] H. Zhao, Z. Jia, W. Yuan, et al., ACS Appl. Mater. Interfaces 7 (2015) 19335–19341.
[16] S. Kadulkar, D.J. Milliron, T.M. Truskett, et al., Phys. Chem. Lett. 11 (2020) 6970–6975.
[17] S. Kadulkar, M.P. Howard, T.M. Truskett, et al., Phys. Chem. B 125 (2021) 4838–4849.
[18] L. Porcarelli, P. Sutton, V. Bocharova, et al., ACS Appl. Mater. Interfaces 13 (2021) 54354–54362.
[19] X.J. Zhang, S. Malhotra, M. Molina, et al., Chem. Soc. Rev. 44 (2015) 1948–1973.
[20] M. Karg, A. Pich, T. Hellweg, et al., Langmuir 35 (2019) 6231–6255.
[21] P. Gurnani, S. Perrier, Prog. Polym. Sci. 102 (2020) 101209.
[22] W.J. Qian, J. Texter, F. Yan, Chem. Soc. Rev. 46 (2017) 1124–1159.
[23] S.Y. Zhang, Q. Zhuang, M. Zhang, et al., Chem. Soc. Rev. 49 (2020) 1726–1755.
[24] H. Hu, B.S. Wang, B.H. Chen, et al., Prog. Polym. Sci. 134 (2022) 101607.
[25] G.C. Claudio, K. Kremer, C.J. Holm, Chem. Phys. 131 (2009) 094903.
[26] Y. Kohno, H. Ohno, Aust. J. Chem. 65 (2012) 91–94.
[27] Y.J. Men, X.H. Li, M. Antonietti, et al., Polym. Chem. 3 (2012) 871–873.
[28] S.M. Chen, Y.H. Peng, Q.S. Wu, et al., Polym. Chem. 7 (2016) 5463–5473.
[29] S. Chen, J. Zheng, D. Mei, et al., Adv. Mater. 30 (2018) 1706102.
[30] H. Wang, M. Matsui, H. Kuwata, et al., Nat. Commun. 8 (2017) 15106.
[31] N. Sahiner, A.O. Yasar, Fuel Process. Technol. 152 (2016) 316–324.
[32] C. Wu, J. Polym. Sci., Part B: Polym. Phys. 32 (1994) 1503–1509.
[33] S. Romer, F. Scheffold, P. Schurtenberger, Phys. Rev. Lett. 85 (2000) 4980–4983.
[34] H.M. Shewan, J.R. Stokes, J. Colloid Interface Sci. 442 (2015) 75–81.
[35] U. Kazuhide, T. Hiroyuki, W. Masayoshi, Phys. Chem. Chem. Phys. 12 (2010) 1649–1658.
[36] O. Nordness, J.F. Brennecke, Chem. Rev. 120 (2020) 12873–12902.
[37] X.F. Wang, H.J. Qiu, Q.S. Wu, et al., ACS Macro Lett. 9 (2020) 1611–1616.
[38] W.M. Haynes, CRC Handbook of Chemistry and Physics, 97th, CRC Press, Boca Raton, Florida, 2016.
[39] J.P. Hansen, I.R. McDonald, Theory of Simple Liquids, Academic Press, London, 2006.
[40] K. Ogawa, A. Nakayama, E. Kokufuta, Langmuir 19 (2003) 3178–3184.
[41] M. Shibayama, T. Tanaka, Adv. Polym. Sci. 109 (1993) 1–62.
[42] J. Brijitta, P. Schurtenberger, Colloid Interface Sci. 40 (2019) 87–103.
[43] A.S. Carreira, F.A.M.M. Gonçalves, P.V. Mendonça, et al., Carbohydr. Polym. 80 (2010) 618–630.
[44] C. Ancla, V. Lapeyre, I. Gosse, et al., Langmuir 27 (2011) 12693–12701.
[45] M.M. Zhou, F. Lu, X.M. Jiang, et al., Polym. Chem. 6 (2015) 8306–8318.
[46] K. Sun, A.K. Matarassoet, R.M. Epler, et al., J. Electrochem. Soc. 165 (2018) A416.
[47] D. Eroglu, K.R. Zavadil, K.G. Gallagher, J. Electrochem. Soc. 162 (2015) A982.
[48] M. Hagen, D. Hanselmann, K. Ahlbrecht, et al., Adv. Energy Mater. 5 (2015) 1401986.
[49] L.X. Li, A.P. Chang, Y.M. Hu, et al., Chem. Commun. 49 (2013) 6534–6536.
[50] Y.L. Jie, X.D. Ren, R.G. Cao, et al., Adv. Funct. Mater. 30 (2020) 1910777.
[51] H.S. Wang, Z.A. Yu, X. Kong, et al., Joule 6 (2022) 588–616.
[52] P. Zhou, X.K. Zhang, Y. Xiang, et al., Nano Res. 16 (2023) 8055–8071.